

Pyrolysis of Biomass Pineapple Residue and Banana Pseudo-Stem: Kinetics, Mechanism and Valorization of Bio-Char

Xin Wang ^{1,*}, Shuo Yang ¹, Boxiong Shen ^{2,*}, Jiancheng Yang ¹ and Lianfei Xu ¹

¹ Tianjin Key Laboratory of Clean Energy and Pollution Control, School of Energy and Environmental Engineering, Hebei University of Technology, Tianjin 300401, China; yangshuonh@126.com (S.Y.); yangjich1023@hebut.edu.cn (J.Y.); xulianfei2006@126.com (L.X.)

² School of Chemical Engineering, Hebei University of Technology, Tianjin 300401, China

* Correspondence: Author: wangxinnh@hebut.edu.cn (X.W.); shenbx@hebut.edu.cn (B.S.); Tel.022-60435279 (X.W.); Fax: 022-60435279 (X.W.)

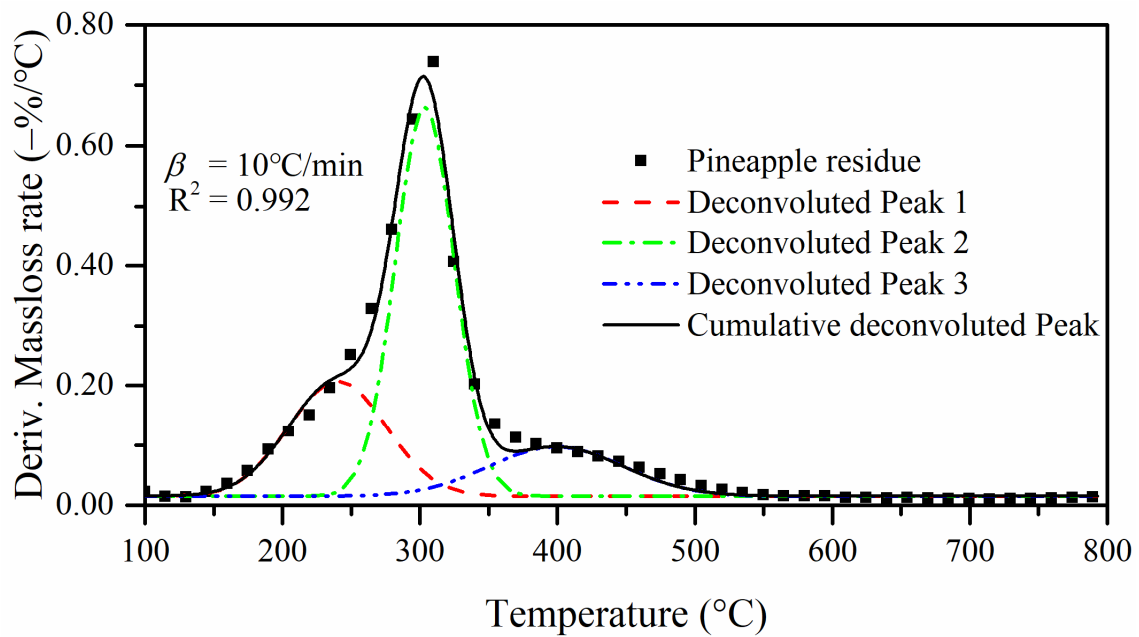


Figure S1. Peak deconvolution of DTG curves of pineapple residue at a heating rate of $10^{\circ}\text{C}/\text{min}$.

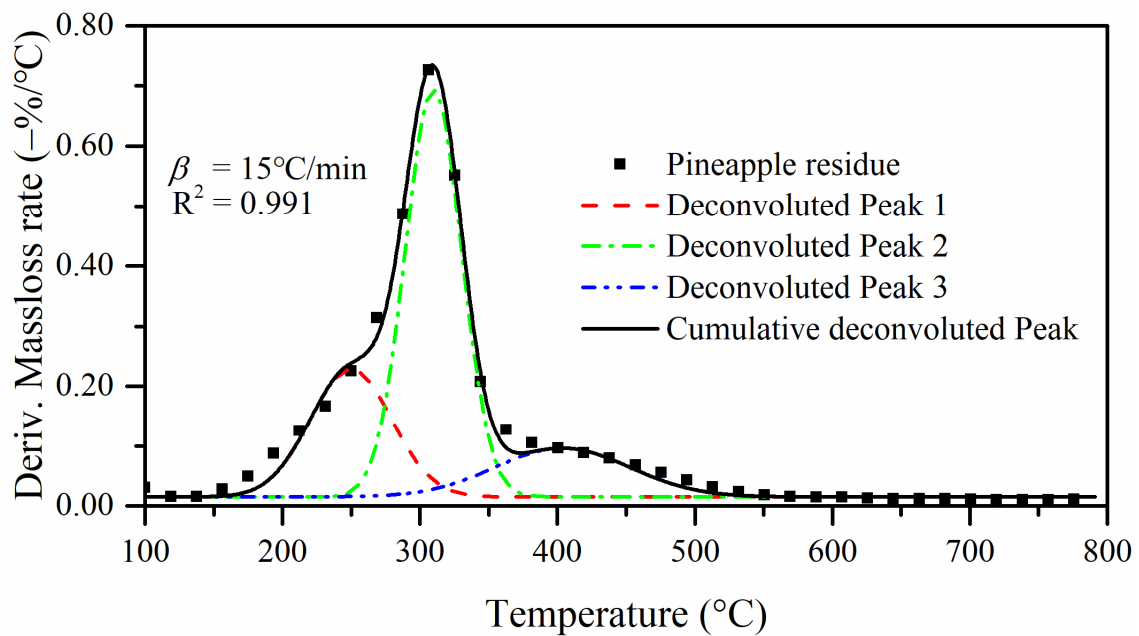


Figure S2. Peak deconvolution of DTG curves of pineapple residue at a heating rate of $15^{\circ}\text{C}/\text{min}$

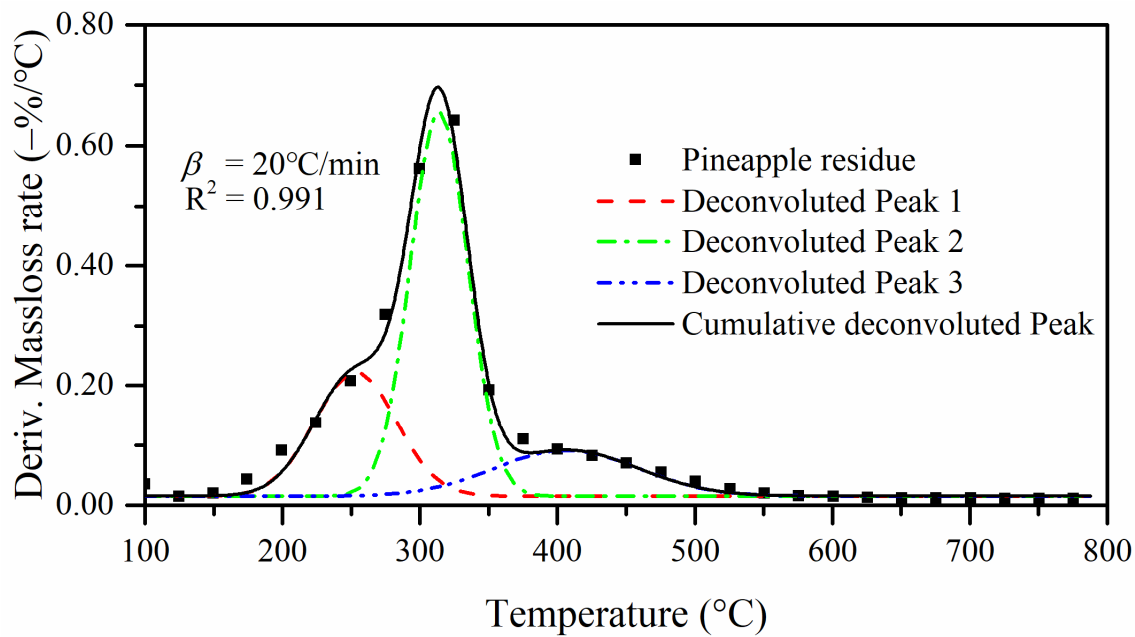


Figure S3. Peak deconvolution of DTG curves of pineapple residue at a heating rate of $20^{\circ}\text{C}/\text{min}$

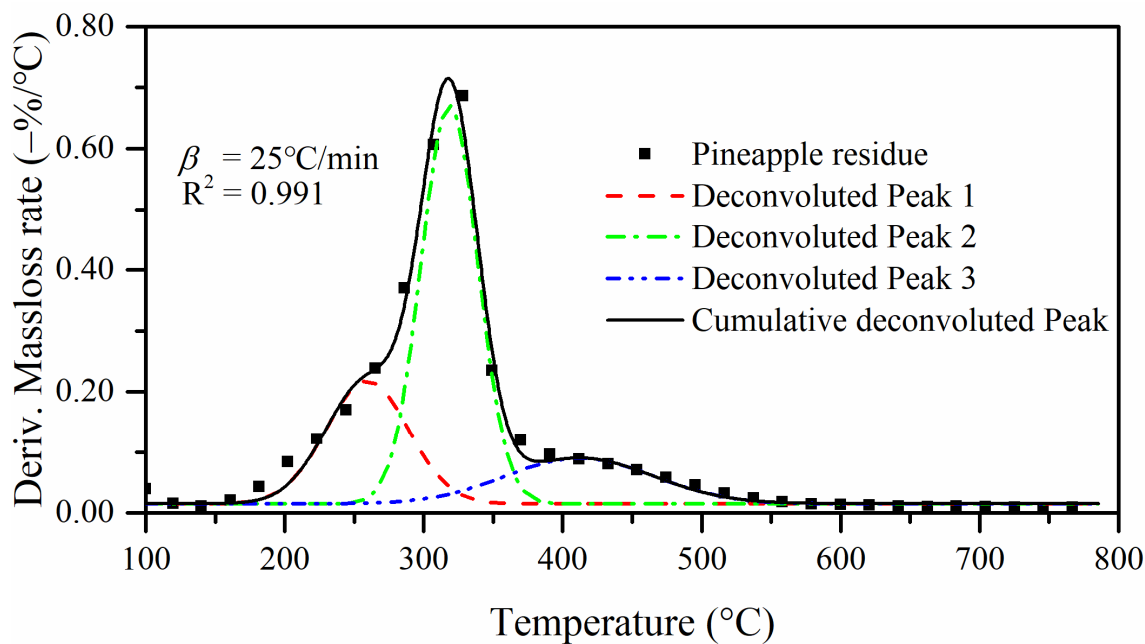


Figure S4. Peak deconvolution of DTG curves of pineapple residue at a heating rate of $25^{\circ}\text{C}/\text{min}$

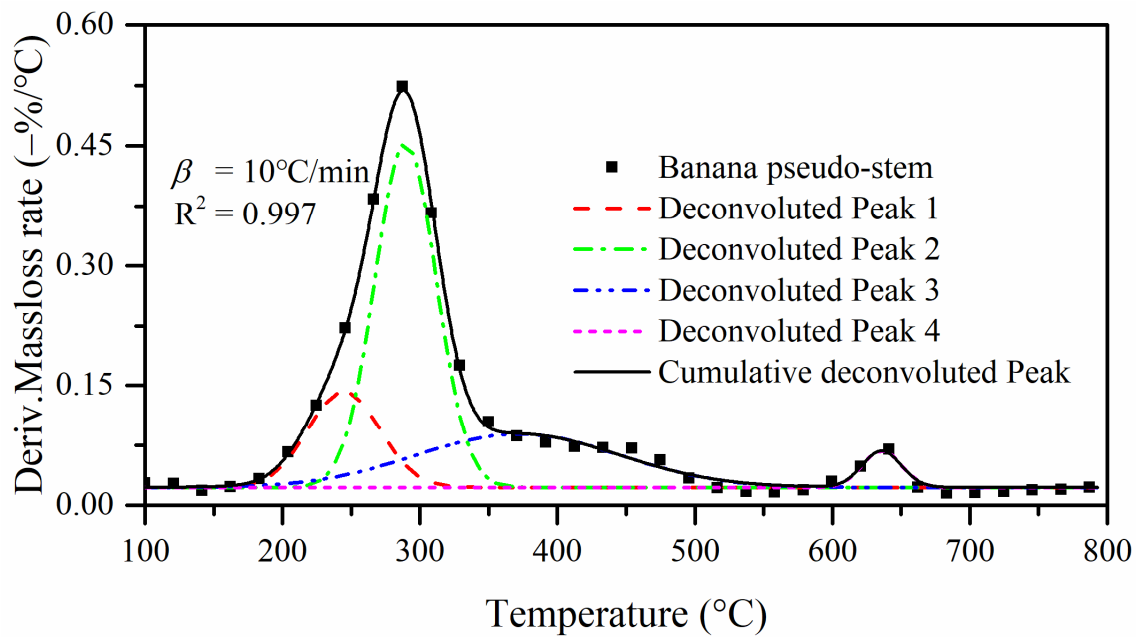


Figure S5. Peak deconvolution of DTG curves of banana pseudo-stem at a heating rate of $10^\circ\text{C}/\text{min}$

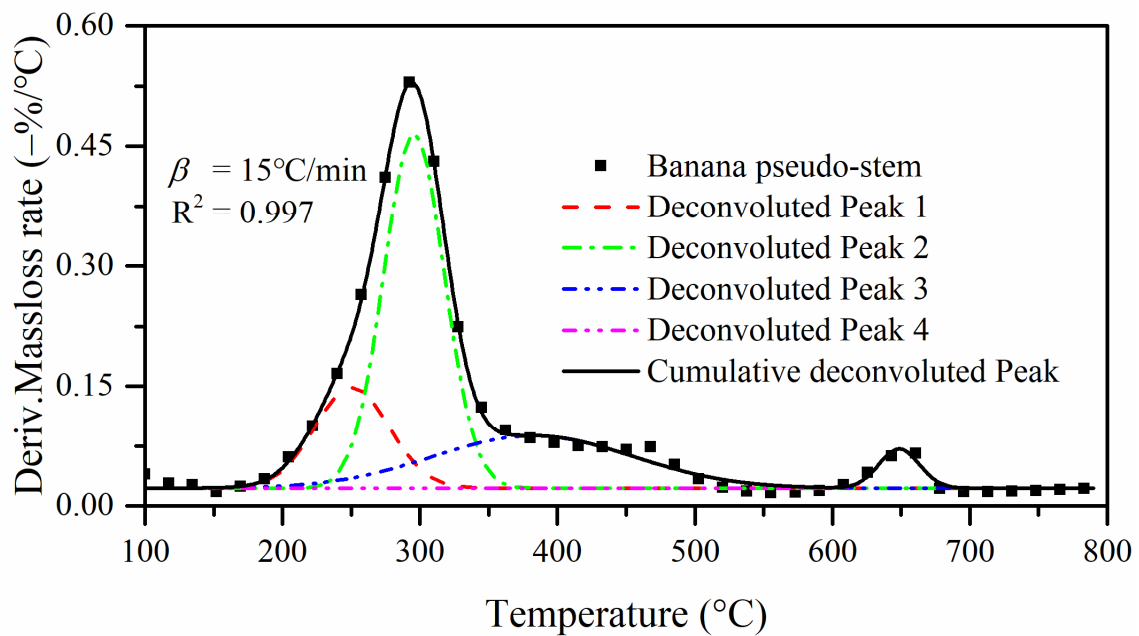


Figure S6. Peak deconvolution of DTG curves of banana pseudo-stem at a heating rate of $15^\circ\text{C}/\text{min}$

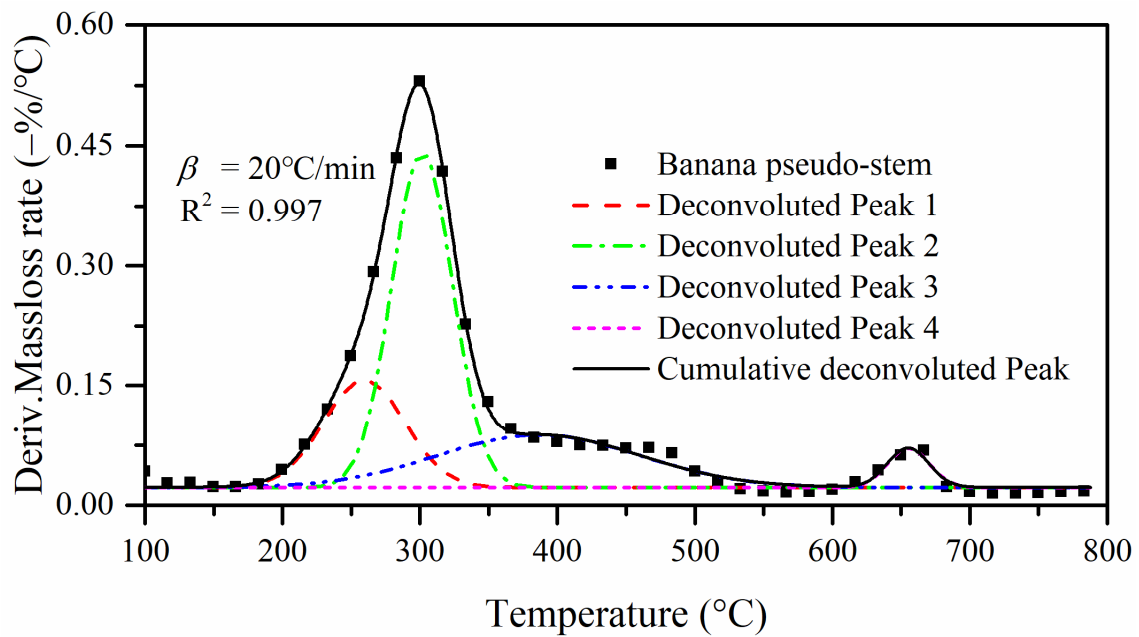


Figure S7. Peak deconvolution of DTG curves of banana pseudo-stem at a heating rate of $20^{\circ}\text{C}/\text{min}$

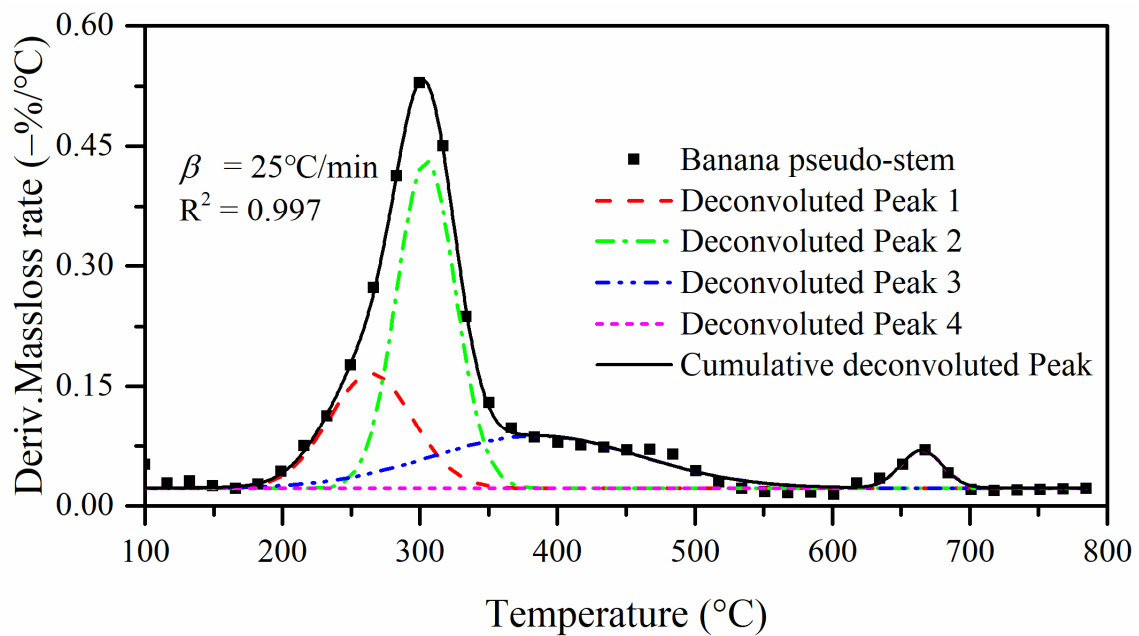


Figure S8. Peak deconvolution of DTG curves of banana pseudo-stem at a heating rate of $25^{\circ}\text{C}/\text{min}$

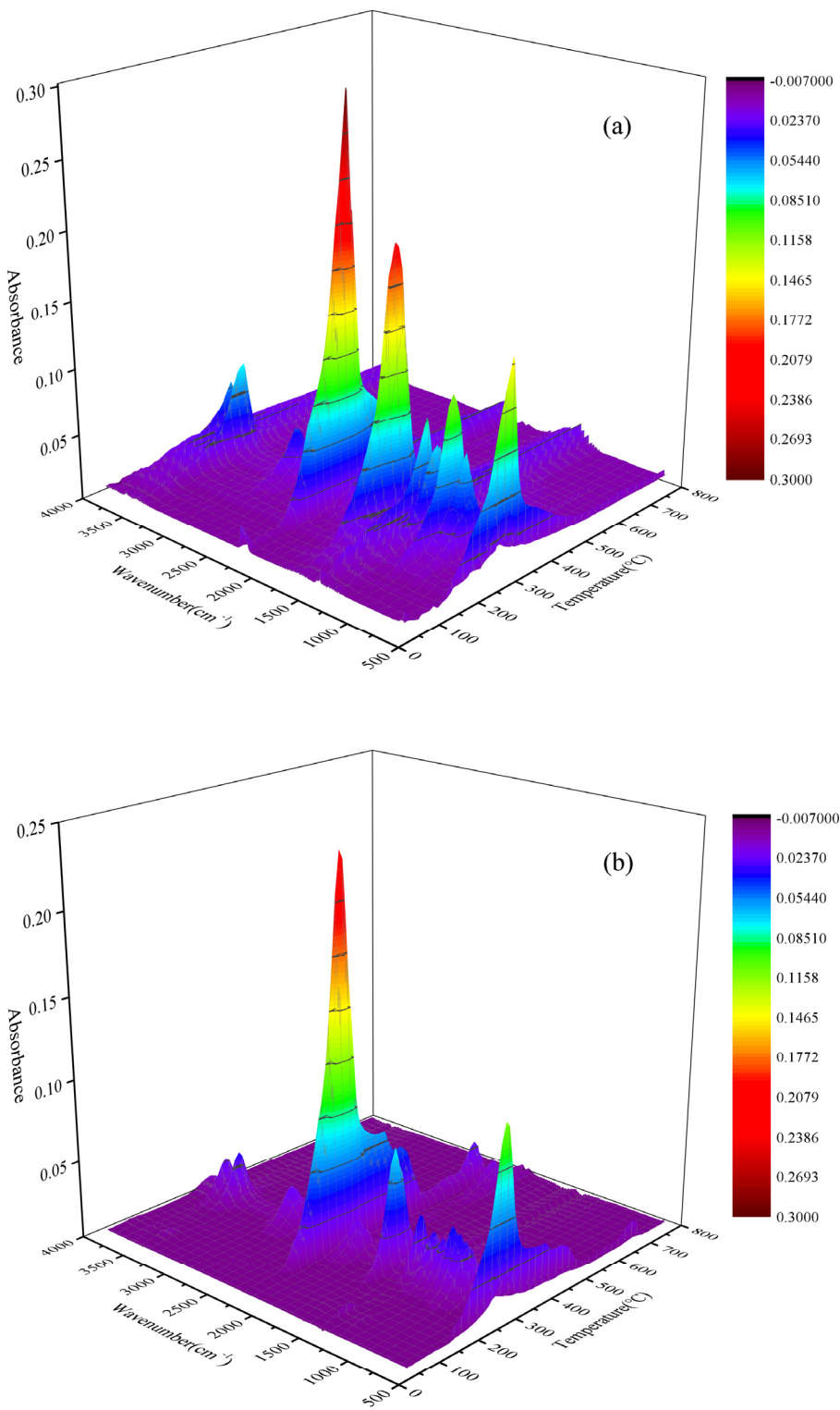


Figure S9. Three-dimensional FTIR distribution of evolved gas during pyrolysis ((a) pineapple residue and (b) banana pseudo-stem)

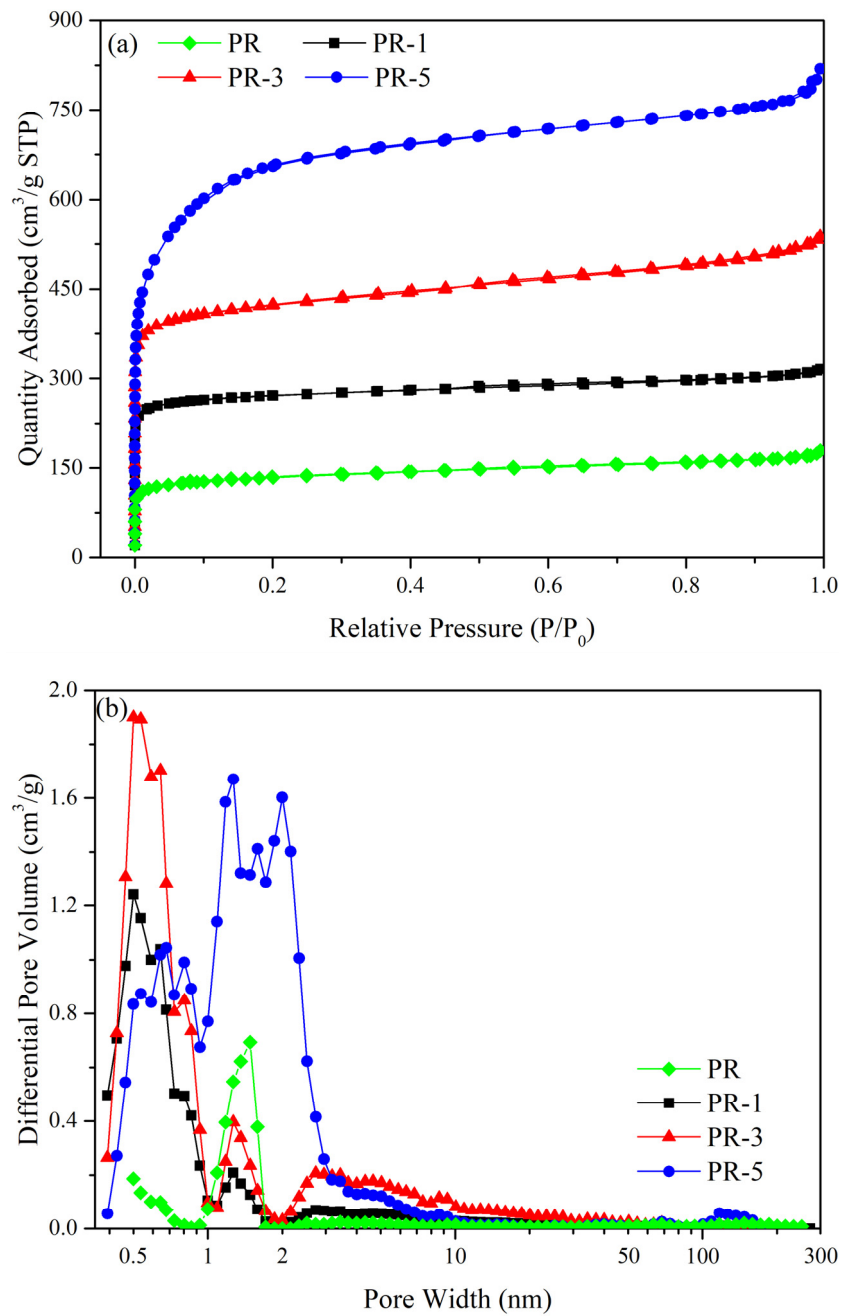


Figure S10. (a) N₂ adsorption-desorption isotherms and (b) pore distribution of biochars and porous carbons sourced from pineapple residue

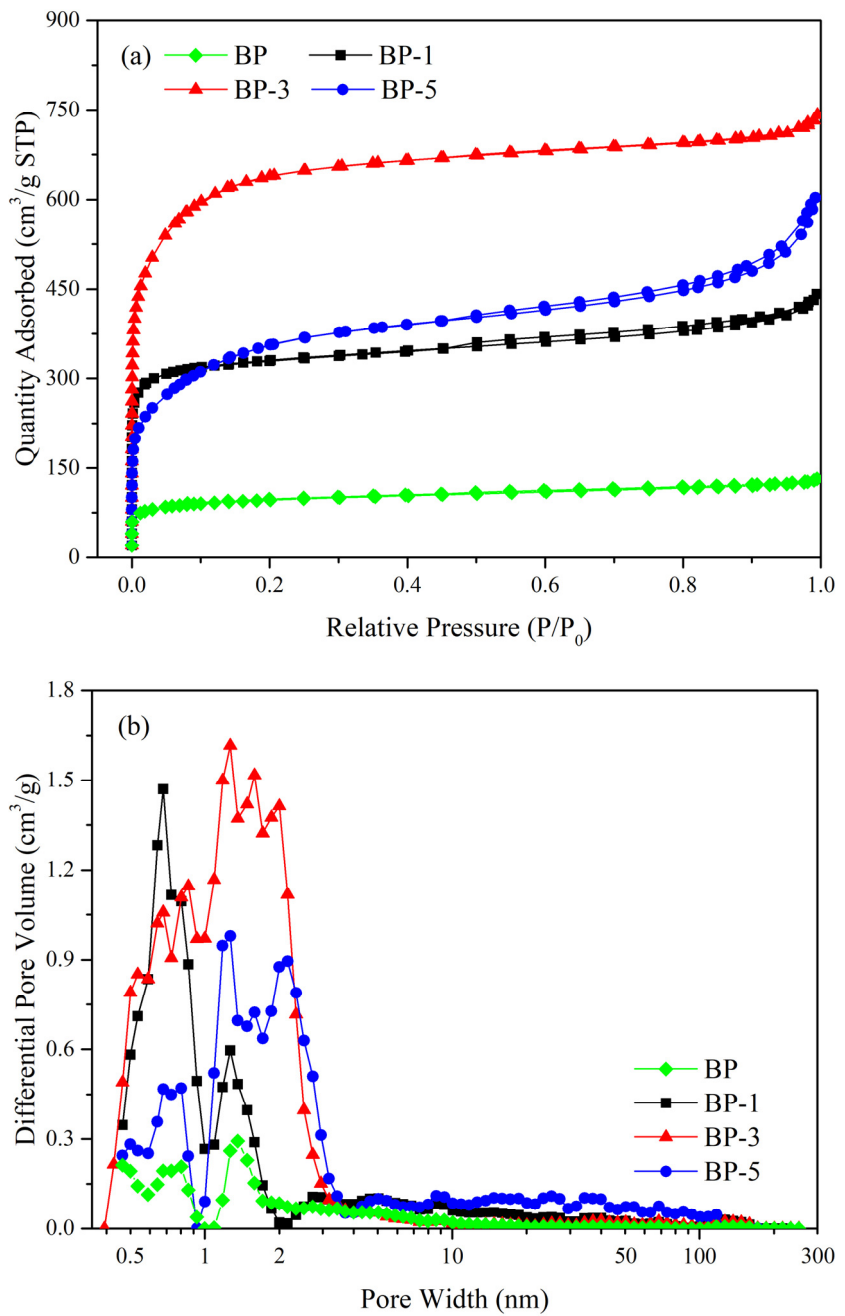


Figure S11. (a) N₂ adsorption-desorption isotherms and (b) pore distribution of biochars and porous carbons sourced from banana pseudo-stems

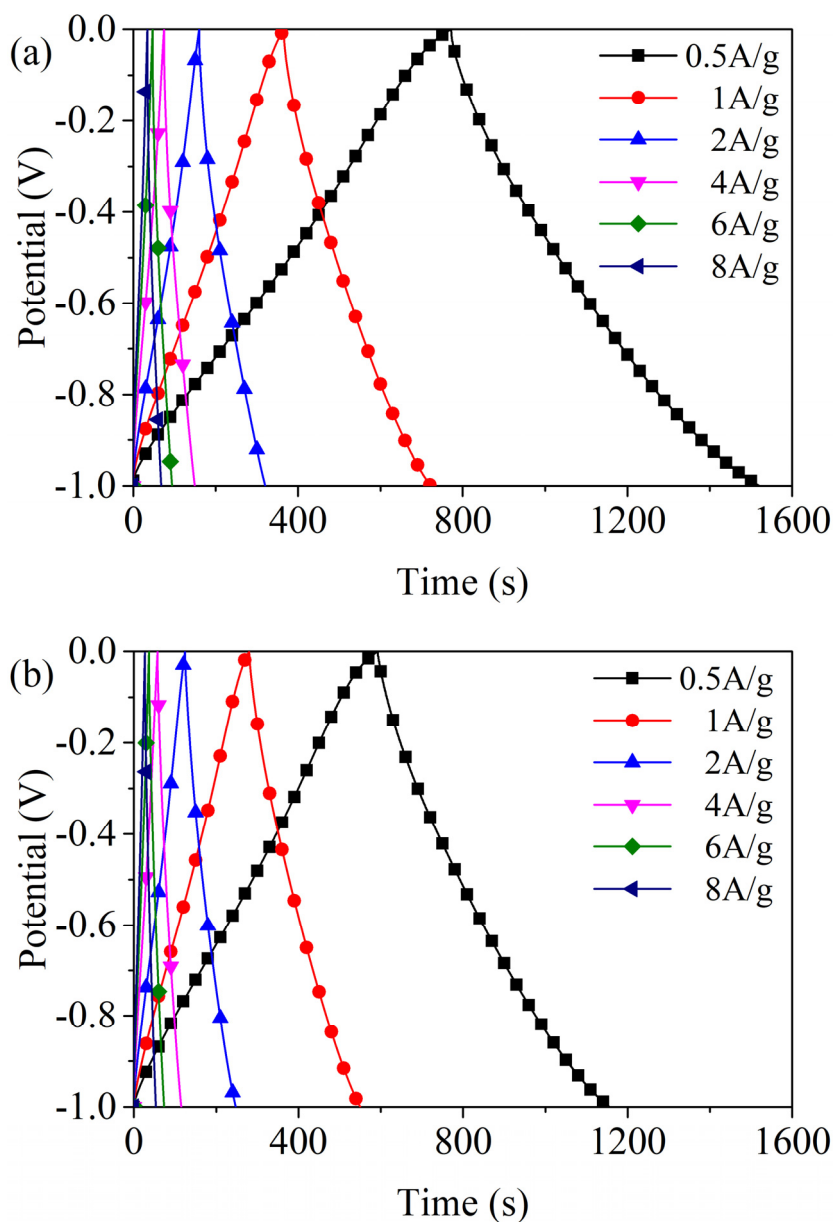


Figure S12. Galvanostatic charge/discharge (GCD) curves of (a) PR-5 and (b) BP-3 at different current densities

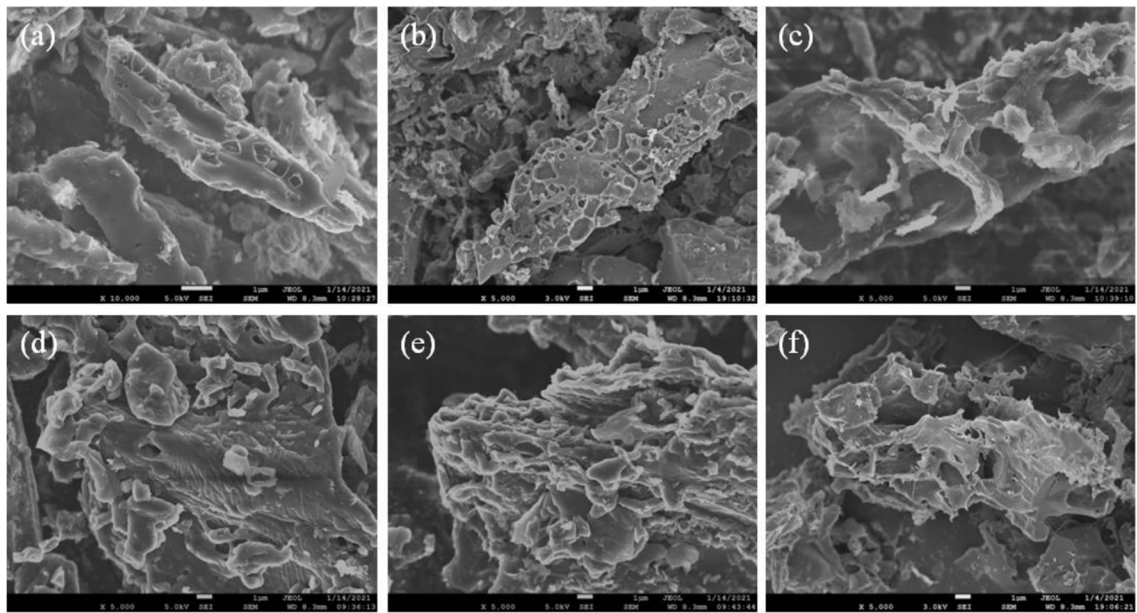


Figure S13. SEM images of porous carbon sourced from pineapple residue and banana pseudo-stem (a) BP-1; (b) BP-3; (c) BP-5; (d) PR-1; (e) PR-3; (f) PR-5

Table S1. Pyrolysis mechanism function

No.	Function Name	Mechanism	$f(\alpha)$
1	Parabolic Law	One-dimensional diffusion, 1D, D ₁ , Deceleration shaped α -t curves	$\frac{1}{2}\alpha^{-1}$
2	Valensi Equation	Two-dimensional diffusion, Cylindrical symmetry, 2D, D ₂ , Deceleration shaped α -t curves	$[-\ln(1-\alpha)]^{-1}$
3	Jander Equation	Two-dimensional diffusion, 2D, $n=1/2$	$4(1-\alpha)^{\frac{1}{2}} \left[1-(1-\alpha)^{\frac{1}{2}} \right]^{-1}$
4	Jander Equation	Two-dimensional diffusion, 2D, $n=2$	$(1-\alpha)^{\frac{1}{2}} \left[1-(1-\alpha)^{\frac{1}{2}} \right]^{-1}$
5	Jander Equation	Three-dimensional diffusion, 3D, $n=1/2$	$6(1-\alpha)^{\frac{2}{3}} \left[1-(1-\alpha)^{\frac{1}{3}} \right]^{\frac{1}{2}}$
6	Jander Equation	Three-dimensional diffusion, Spherically symmetric, 3D, D ₃ , Deceleration shaped α -t curves, $n=2$	$\frac{3}{2}(1-\alpha)^{\frac{2}{3}} \left[1-(1-\alpha)^{\frac{1}{3}} \right]^{-1}$
7	Ginstling-Brounshtein Equation	Three-dimensional diffusion, Spherically symmetric, 3D, D ₄ , Deceleration shaped α -t curves	$\frac{3}{2} \left[(1-\alpha)^{-\frac{1}{3}} - 1 \right]^{-1}$

8	Anti-Jander Equation	Three-dimensional diffusion, 3D	$\frac{3}{2}(1+\alpha)^{\frac{2}{3}} \left[(1+\alpha)^{\frac{1}{3}} - 1 \right]^{-1}$
	Z.-L.-T. Equation	Three-dimensional diffusion, 3D	$\frac{3}{2}(1-\alpha)^{\frac{4}{3}} \left[(1-\alpha)^{-\frac{1}{3}} - 1 \right]^{-1}$
10	Avrami-Erofeev Equation	Random nucleation and subsequent growth, A4, S-shaped α -t curves	$4(1-\alpha)[- \ln(1-\alpha)]^{\frac{3}{4}}$
11	Avrami-Erofeev Equation	Random nucleation and subsequent growth, A3, S-shaped α -t curves, $n = 1/3, m=3$	$3(1-\alpha)[- \ln(1-\alpha)]^{\frac{2}{3}}$
12	Avrami-Erofeev Equation	Random nucleation and subsequent growth, $n=2/5$	$\frac{5}{2}(1-\alpha)[- \ln(1-\alpha)]^{\frac{3}{5}}$
13	Avrami-Erofeev Equation	Random nucleation and subsequent growth, A2, S-shaped α -t curves, $n=1/2, m=2$	$2(1-\alpha)[- \ln(1-\alpha)]^{\frac{1}{2}}$
14	Avrami-Erofeev Equation	Random nucleation and subsequent growth, $n=2/3$	$\frac{3}{2}(1-\alpha)[- \ln(1-\alpha)]^{\frac{1}{3}}$
15	Avrami-Erofeev Equation	Random nucleation and subsequent growth, $n=3/4$	$\frac{4}{3}(1-\alpha)[- \ln(1-\alpha)]^{\frac{1}{4}}$
16	Mample Single-line rule, first order	Random nucleation and subsequent growth, Assuming each particle has only one core, A1, F1, S-shaped α -t curves, $n=1, m=1$	$1-\alpha$
17	Avrami-Erofeev Equation	Random nucleation and subsequent growth, $n=3/2$	$\frac{2}{3}(1-\alpha)[- \ln(1-\alpha)]^{-\frac{1}{2}}$
18	Avrami-Erofeev Equation	Random nucleation and subsequent growth, $n=2$	$\frac{1}{2}(1-\alpha)[- \ln(1-\alpha)]^{-1}$

19	Avrami-Erofeev Equation	Random nucleation and subsequent growth, $n=3$	$\frac{1}{3}(1-\alpha)[- \ln(1-\alpha)]^{-2}$
20	Avrami-Erofeev Equation	Random nucleation and subsequent growth, $n=4$	$\frac{1}{4}(1-\alpha)[- \ln(1-\alpha)]^{-3}$
21	P.-T. Equation	Autocatalytic reaction, Dendritic nucleation, Au, B1 (S-shaped α -t curves)	$\alpha(1-\alpha)$
22	Mampel Power Law	$n=1/4$	$4\alpha^{\frac{3}{4}}$
23	Mampel Power Law	$n=1/3$	$3\alpha^{\frac{2}{3}}$
24	Mampel Power Law	$n=1/2$	$2\alpha^{\frac{1}{2}}$
25	Mampel Power Law	Phase boundary reaction (One-dimensional), R1, $n=1$	1
26	Mampel Power Law	$n=\frac{3}{2}$	$\frac{2}{3}\alpha^{-\frac{1}{2}}$
27	Mampel Power Law	$n=2$	$\frac{1}{2}\alpha^{-1}$
28	Reaction order	$n=1/4$	$4(1-\alpha)^{\frac{3}{4}}$
29	Contraction globular (Volume)	Phase boundary reaction, Spherically symmetric, R3, Deceleration shaped α -t curves, $n=1/4$	$3(1-\alpha)^{\frac{2}{3}}$
30		$n=3$ (Three-dimensional)	$(1-\alpha)^{\frac{2}{3}}$

31	Contraction of the cylinder (Area)	Phase boundary reaction, Cylindrical symmetry, R2, Deceleration shaped α -t curves, $n=1/2$	$2(1-\alpha)^{\frac{1}{2}}$
32		$n=2$ (Two-dimensional)	$(1-\alpha)^{\frac{1}{2}}$
33	Reaction order	$n=2$	$\frac{1}{2}(1-\alpha)^{-1}$
34	Reaction order	$n=3$	$\frac{1}{3}(1-\alpha)^{-2}$
35	Reaction order	$n=4$	$\frac{1}{4}(1-\alpha)^{-3}$
36	Two order	Chemical reaction, F2, Deceleration shaped α -t curves	$(1-\alpha)^2$
37	2/3 order	Chemical reaction	$2(1-\alpha)^{\frac{3}{2}}$
38	Exponential Law	E1, $n=1$, Accelerated shaped α -t curves	α
39	Exponential Law	$n=2$	$\frac{1}{2}\alpha$
40	Three order	Chemical reaction, F3, Deceleration shaped α -t curves	$\frac{1}{2}(1-\alpha)^3$

Table S2. Pyrolysis thermodynamic parameters of the deconvoluted peaks

Deconvoluted peaks	Peak temperature (°C)	Enthalpy ΔH (kJ/mol)	Gibbs free energy ΔG (kJ/mol)	Entropy ΔS (J/mol)
Pineapple residue				
1	233	135	127	16
2	294	182	132	88
3	385	270	170	153
Banana pseudo-stem				
1	232	170	134	72
2	278	171	132	70
3	359	275	172	163
4	618	357	210	165

Table S3. The relative content of main volatile organic compounds sourced from pineapple residue

No.	Time	Compounds	Formula	Relative content (%)
1	2.14	Acetic acid	C ₂ H ₄ O ₂	8.60±0.28
2	2.31	Methyl ethanoate	C ₃ H ₆ O ₂	12.46±0.40
3	2.32	Acetyl ether	C ₄ H ₆ O ₃	30.41±0.97
4	2.72	2-Heptynoic acid	C ₇ H ₁₀ O ₂	1.56±0.05
5	2.82	1-Acetoxy-2-butanone	C ₆ H ₁₀ O ₃	6.27±0.20
6	2.91	Succindialdehyde	C ₄ H ₆ O ₂	3.02±0.10
7	3.35	Furfural	C ₅ H ₄ O ₂	8.21±0.26
8	3.50	Furfuryl alcohol	C ₅ H ₆ O ₂	2.33±0.07
9	3.60	Acetonyl acetate	C ₅ H ₈ O ₃	4.03±0.13
10	4.07	2-Methyl-2-cyclopenten-1-one	C ₆ H ₈ O	0.68±0.02
11	4.14	Butyrolactone	C ₄ H ₆ O ₂	3.42±0.11
12	4.28	2-Cyclopenten-1-one, 2-hydroxy	C ₅ H ₆ O ₂	3.07±0.10
13	4.71	1-Acetoxy-2-butanone	C ₆ H ₁₀ O ₃	0.88±0.03
14	4.80	3-Methyl-2-cyclopentenone	C ₆ H ₈ O	0.43±0.01
15	4.94	Phenol	C ₆ H ₆ O	1.65±0.05
16	5.29	Tetrahydro-2-furanmethanol	C ₅ H ₁₀ O ₂	0.55±0.02
17	5.57	3-Methyl-1,2-cyclopentanedione	C ₆ H ₈ O ₂	1.58±0.05
18	6.46	2-Methoxyphenol	C ₇ H ₈ O ₂	1.53±0.05
19	6.52	4-Ethyl-2-hydroxy-2-cyclopentenone	C ₇ H ₁₀ O ₂	0.56±0.02
20	6.59	Cyclopropyl carbinol	C ₄ H ₈ O	3.97±0.13

21	6.85	2-Methyl-1,3-cyclohexanedione	C ₇ H ₁₀ O ₂	0.59±0.02
22	8.28	2,3-Dihydro-1-benzofuran	C ₈ H ₈ O	2.09±0.07
23	8.56	1,2,3-Propanetriol,1-acetate	C ₅ H ₁₀ O ₄	0.60±0.02
24	9.59	2-Methoxy-4-vinylphenol	C ₉ H ₁₀ O ₂	1.52±0.05

Table S4. The relative content of main volatile organic compounds sourced from banana pseudo-stem

No.	Time	Compounds	Formula	Relative content (%)
1	2.10	Acetic acid	C ₂ H ₄ O ₂	33.71±1.08
2	2.30	Hydroxyacetone	C ₃ H ₆ O ₂	36.02±1.15
3	2.70	2-Heptynoic acid	C ₇ H ₁₀ O ₂	0.56±0.02
4	2.81	3-Pentanone	C ₅ H ₁₀ O	3.47±0.11
5	2.91	Methyl valeraldehyde	C ₆ H ₁₂ O	1.20±0.04
6	3.33	Furfural	C ₅ H ₄ O ₂	6.17±0.20
7	3.50	Methylenecyclopropanecarboxylic acid	C ₅ H ₆ O ₂	1.85±0.06
8	3.60	2-Propanone, 1-(acetoxy)-	C ₅ H ₈ O ₃	1.23±0.04
9	4.07	2-methylcyclopent-2-en-1-one	C ₆ H ₈ O	0.69±0.02
10	4.15	Butanoic acid,4-hydroxy-	C ₄ H ₈ O ₃	2.92±0.09
11	4.27	2-Cyclopenten-1-one, 2-hydroxy	C ₅ H ₆ O ₂	0.72±0.02
12	4.93	Phenol	C ₆ H ₆ O	1.23±0.04
13	5.29	Propanoic acid, 2-methyl-, anhydride	C ₈ H ₁₄ O ₃	0.58±0.02
14	5.56	1,2-Cyclopentanedione, 3-methyl	C ₆ H ₈ O ₂	1.22±0.04
15	6.45	Phenol, 2-methoxy	C ₇ H ₈ O ₂	1.46±0.05
16	6.59	Cyclopropyl carbinol	C ₄ H ₈ O	3.92±0.13
17	8.28	Benzofuran, 2,3-dihydro	C ₈ H ₈ O	1.40±0.04
18	9.59	2-Methoxy-4-vinylphenol	C ₉ H ₁₀ O ₂	0.77±0.02
19	10.06	Phenol, 2,6-dimethoxy	C ₈ H ₁₀ O ₃	0.88±0.03